Materials and Structures (2017) 50:50
DOI 10.1617/s11527-016-0877-6

ORIGINAL ARTICLE

Response of alkali activated low calcium fly-ash based geopolymer concrete under compressive load at elevated temperatures

M. Talha Junaid · Obada Kayali · Amar Khennane

Received: 9 February 2016 / Accepted: 19 April 2016 / Published online: 11 August 2016

Abstract For geopolymer cement (GPC) concrete to become a viable building material in the main stream construction industry, reliable stress–strain curves need to be established. This paper presents the stress–strain curves for GPC concrete at ambient and elevated temperatures of up to 800 °C. Prediction models for capturing the stress–strain response of GPC concrete at ambient temperatures, based on widely accepted OPC models, are also presented here. At high temperatures testing only covered one type of temperature-load history; that is: samples were heated up to test temperatures then loaded to failure under displacement control. Between 20 and 200 °C all the tested samples underwent a decrease in strength. However, samples tested between 200 and 400 °C manifested a moderate to significant gain in strength. At 800 °C all samples underwent a decrease in strength. The initial loss of strength may be attributed to the loss of water from the GPC concrete samples, which is supported by thermogravimetric analysis of geopolymer samples. Between 200 and 400 °C, the increase in the compressive strength of all tested concrete mixtures is attributed to further geopolymerization, which has been proven by differential scanning calorimetry results. The loss of strength at 800 °C is attributed to possible disintegration of the geopolymer gel and formation of new phases within the geopolymer system.

Keywords Geopolymer concrete · Stress–strain curves · Alkali activated fly ash concrete · Flashag · Elevated temperature · Elastic modulus

M. Talha Junaid (✉)
Department of Civil and Environmental Engineering, College of Engineering, University of Sharjah, Sharjah, UAE
e-mail: mjunaid@sharjah.ac.ae

O. Kayali · A. Khennane
School of Engineering and Information Technology, UNSW Canberra, Northcott Drive, Campbell, ACT 2600, Australia

1 Introduction

Alkali liquids (usually a soluble metal hydro-oxide and/or alkali silicate) are usually used to react with silica (SiO_2) and alumina (Al_2O_3) rich natural materials, like metakaolin or with industrial by-products, such as fly ash (FA), silica fume (SF), rice husk ash (RHA) or slag to produce binders [1–4]. Such alkali activated binders made using low calcium source material, such as class F fly ash, are generally referred to as geopolymer cement (GPC) concrete or simply geopolymer concrete [5]. The strength development of GPC binders does not rely on the hydration of Portland cement; production of which primarily depends on calcining limestone, a major source of CO_2 emission in ordinary portland cement (OPC) concrete. GPC can hence reduce emissions by 45–80 % for each cubic

metre of OPC concrete replaced [4, 6]. In the last decade, or so, extensive research has been undertaken with the view to industrialise GPC, as an alternative to OPC concrete for more sustainable construction.

Research thus far suggests that GPC has better resistance to fire than OPC concrete [6–17]. However, most of this research focuses on the residual properties of GPC concrete and very limited information is available on the at-temperature properties of GPC. Pan and Sanjayan [16] reported on stress–strain behaviour of GPC pastes at elevated temperatures and the variation of the at-temperature and residual strength. This work revealed that the at-temperature response of GPC is significantly different from the residual response. But, the effect of aggregates characteristics on the at-temperature properties has hardly been reported. Shaikh and Vimonsatit [17] reported the effect of molarities, curing regimes and aggregate size on the at-temperature strength properties of low calcium fly ash based GPC concretes, but the stress–strain history was not captured. Limited data [18–21] are available on the presence of transient creep in GPC specimen and the characterization of the deformational behaviour of GPC concrete while at elevated temperature, especially its stress–strain behaviour.

As fire engineering moves towards a performance based approach, many codes, in addition to the nominal (standard) fire resistance rating of individual elements, require a full analysis of the structure, which is not possible without prior knowledge of the evolution of the thermal and mechanical properties with temperature. Moreover, any such analysis will require constitutive material models for GPC concrete. Such a constitutive model for GPC is currently not available, and the development of which requires understanding the stress–strain behaviour of GPC for a wide range of load-temperature histories.

It is imperative, therefore, that the stress–strain response in compression of such concretes while at high temperatures be captured; hence the focus of this study.

2 Materials and mixes

For the purpose of determining the stress–strain behaviour of GPC concrete at elevated temperatures, three GPC mixes were used with nominal strength of 40, 50 and 60 MPa. The mix design was carried out using the methodology and framework proposed by Junaid et al. [22]. Tests were conducted at ambient temperature as well as at 100, 200, 300, 400 and 800 °C. The composition of the three different mixes containing two different types of aggregates; typical basalt natural aggregates and non-pelletized light weight fly ash (Flashag) aggregates are shown in Table 1. Flashag aggregates were manufactured using only sintered fly ash and crushing the product into suitable sizes [23].

The designed mixes and curing conditions are given in Table 1 along with the ambient strength and elastic modulus. The rest period of mixes M7 and M14 was 24 h while that of M4SP was increased to 72 h to ensure it reached a nominal strength of 50 MPa. Cylindrical samples whose nominal dimensions are 75 mm diameter × 150 mm height were used in these tests. All tests were conducted 7 days after casting of concrete. Mixes M7 and M14 contained natural aggregates while M4-SP contained artificial non-pelletized fly ash aggregates. The tests were carried out using the relevant Australian Standards respectively for strength and elastic modulus [24, 25].

Laboratory grade D sodium silicate solution with SiO_2/Na_2O between 1.95 and 2.05 was procured from IMCD Australia Limited. Sodium Hydroxide solutions (12 M) were made from 98 % purity NaOH flakes supplied by Redox Pyt Ltd., Australia. The composition of FA used in the study as determined by X-ray Fluorescence (XRF) is tabulated in Table 2.

2.1 Testing regime

In addition to ambient temperatures, the behaviour of GPC concrete was also studied at the higher temperatures of 100, 200, 300, 400 and 800 °C. These temperatures are important since at 100 °C the movement of water in the GPC system will affect its properties, while it has been reported that between 200 and 400 °C further geopolymerization occurs [11, 12, 15, 16, 26–28]. At 800 °C disintegration of the geopolymer gel as well as phase changes within the gel are reported in addition to densification and contraction of the matrix [8, 29, 30] and is thus of interest for this investigation.

At ambient temperatures, standard tests were conducted to measure the strength and elastic modulus of GPC samples under load control regimes, using a 3000 kN Technotest machine. The load rate for the

Table 1 Mix design data for the samples tested

	M7	M14	M4SP
FA (kg/m^3)	420	420	440
NaOH (12 M solution) (kg/m^3)	60	67.6	65
Sodium silicate solution (kg/m^3)	150	169	162.5
Coarse (kg/m^3)	1090	1127	660[a]
Fine (kg/m^3)	574	575	340[a]
Water (kg/m^3)	32.3	0	11
VM & SP[b] (kg/m^3)	8	8	8
f'_c (MPa)	40.2	60.7	48.5
E (GPa)	18.7	25.7	15.2
Density (kg/m^3)	2197	2213	1679
Rest period (h)	24	24	72
Curing	72 h	72 h	72 h
	80 °C	80 °C	80 °C
	Dry heat	Dry heat	Dry heat

[a] Flashag aggregates were used

[b] Viscosity modifier and superplasticizer

Table 2 Chemical composition of fly ash using XRF

Compound	SiO_2	Al_2O_3	Fe_2O_3	CaO	K_2O	TiO_2	MgO	Na_2O	L.O.I
% Composition by weight	62.19	27.15	3.23	1.97	0.89	1.06	0.4	0.3	1.75

compression tests was 0.33 MPa/s while that for elastic modulus tests was 0.25 MPa/s as per the Australian Standards' guidelines. This control data was used to determine the loading rate for displacement control stress–strain response tests, at ambient and elevated temperatures. The displacement control loading rate was kept between 0.15 and 0.20 mm/min. It must be noted that the tests conducted in this study covered only one type of temperature-load histories; that is: the samples were heated until the test temperature is reached and thermal equilibrium achieved (measured using embedded thermocouples) then loaded to failure under displacement control while hot. Heating rates of 5 °C/min [31] was used for all tests as schematically represented in Fig. 1.

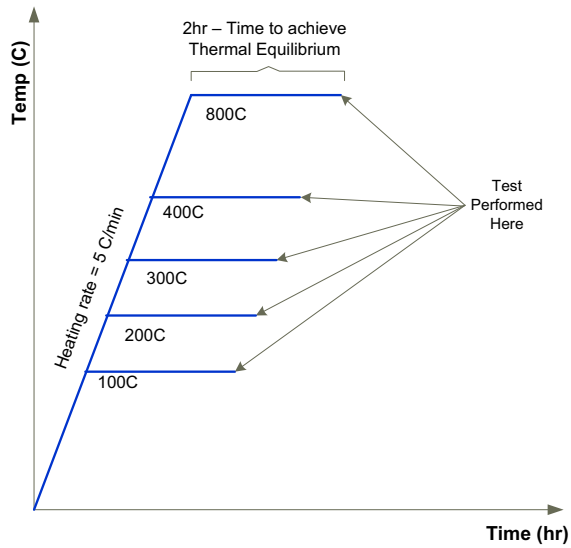

Fig. 1 Heating regime used in this study

3 Results and discussions

3.1 Elastic modulus at ambient temperature

For OPC concrete, Australian Standard 3600-2009 recommends the mean modulus of elasticity for mean compressive strength greater than 40 MPa as:

$$E_c = \rho^{1.5} \times 0.024\sqrt{f'_c} + 0.12 \pm 20\ \% \quad (1)$$

Diaz-Loya et al. [32] has proposed Eq. 2 for the prediction of modulus of elasticity based on average

density (ρ) of GPC in kg/m^3 and the average compressive strength (f_c') in MPa.

$$E_c = 0.037\rho^{1.5}\sqrt{f_c'} \quad (2)$$

Equation 1 reports conservative values for E_c while Eq. 2 overestimate the elastic modulus of GPC concrete samples which can be an issue in practical applications. As evident from Fig. 2, the results obtained from Eq. 1 are conservative and being far below the actual value may compromise economy. Using available data from Diaz-Loya et al. [32], Yifei [33] and the current research, a multiple non-linear regression was performed using the online tool provided by VLab [34] and Eq. 3 is proposed as a relationship between elastic modulus, density and compressive strength of GPC.

$$E_c = 0.015 f_c'^{0.84}\rho^{1.43} \quad (3)$$

The proposed model shows good agreement with published results of GPC concrete with an R^2 value of over 0.78 as compared to just 0.61 for Eq. 2. Using this model decreases the over estimation cases from 75 % (for Eq. 2) to less than 30 % (for Eq. 3). In all cases of over estimation the values predicted by this model are lower than those predicted by Eq. 2. This trend is shown graphically in Fig. 2.

3.2 Stress–strain curves at ambient temperature

Stress strain curves for the three mixes at ambient temperatures are given in Fig. 3. Given the variation in nominal characteristic strength of the three mixes, their stress–strain behaviour is slightly different. Especially of notice is stress–strain relationship of M4SP, which shows a distinct post peak behaviour. The rate of strain development, as well as the strain at maximum stress is significantly different from the other two concrete types. This may largely be due to the fact that M4SP contained artificial lightweight aggregates. To compare the behaviour of these GPC concretes with that of OPC concretes, several existing analytical stress–strain models were studied and compared with the GPC experimental data. These included the models proposed by Anderberg and Thelanderson [35], Tomaszewicz [36], Collins et al. [37], and Sargin and Handa [38]. Among these, the models proposed by Collins et al. [37] and Sargin and Handa [38] most closely predicted the experimental stress–strain behaviour of GPC concretes. Collins

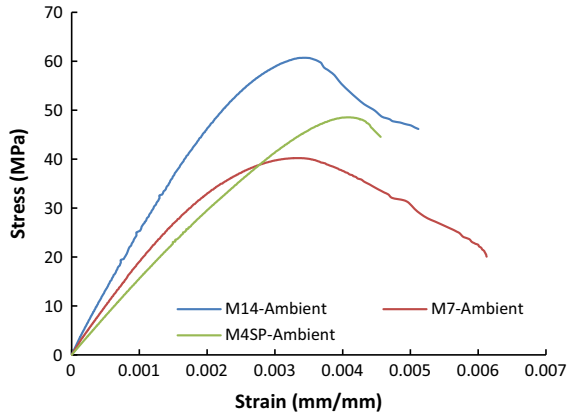

Fig. 3 Stress–strain curves of GPC samples at ambient temperatures

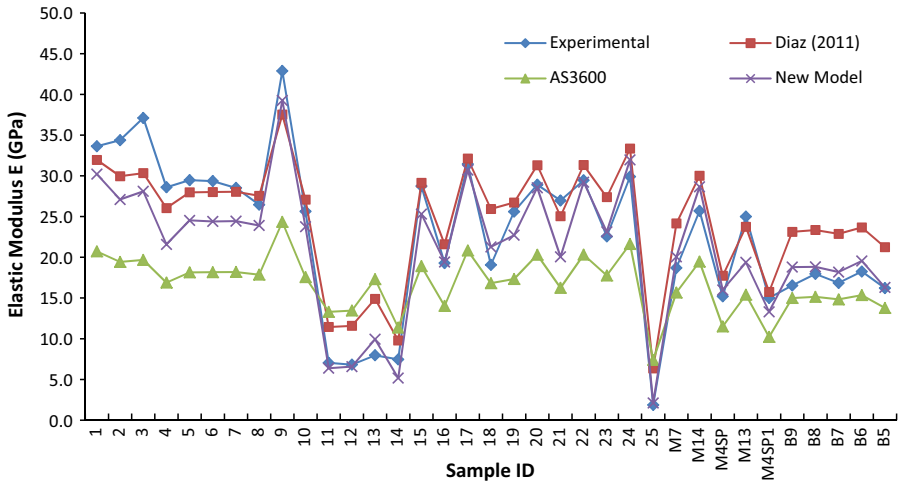

Fig. 2 Comparison of experimental young modulus values with various prediction models

et al. [37] model for stress strain curves for high strength OPC concrete in compression is given by:

$$\sigma_c = f_c' \frac{\varepsilon_c}{\varepsilon_{cm}} \frac{n}{n - 1 + (\varepsilon_c/\varepsilon_{cm})^{nk}} \quad (4)$$

while Sargin and Handa [38] proposed the following model to express the stress strain relationship of OPC concretes.

$$\sigma_c = \frac{A\eta - \eta^2}{1 + (A-2)\eta} f_c' \quad (5)$$

where ε_c = strain at stress σ_c, f_c' = peak compressive stress, ε_{cm} = strain at peak stress $n = 0.8 + (f_c'/17)$, $k = 0.67 + (f_c'/62)$ when $\varepsilon_c/\varepsilon_{cm} > 1$; $k = 1.0$ when $\varepsilon_c/\varepsilon_{cm} \leq 1$, $A = E_{co}/E_c$, $\eta = \varepsilon_c/\varepsilon_{cm}$, E_c = initial tangent modulus or elastic modulus, E_{co} = secant modulus from origin to peak compressive stress

A comparison of the representative stress strain relationship of GPC concrete with the above models for the three types of mixes tested at ambient temperatures are presented in Fig. 4. Although the established Collins and Sargin models provide good prediction for the stress–strain relationship of GPC concrete, the post peak behaviour is not captured accurately. Therefore a new empirical model based on Collins' work is presented here. The stress–strain relationship of GPC concretes in the new model are essentially represented by the Eq. 4 above, however, the k and n factors have been modified empirically in this study to fit the test data for normal and lightweight aggregates and are given below.

For normal aggregates: $n = 0.7 + (f_c'/23)$

$k = 0.6 + (f_c'/86)$ when $\varepsilon_c/\varepsilon_{cm} > 1$
$= 1.0$ when $\varepsilon_c/\varepsilon_{cm} \leq 1$

For Flashag/lightweight aggregates: $n = 0.72 + (f_c'/11)$

$k = 0.6 + (f_c'/70)$ when $\varepsilon_c/\varepsilon_{cm} > 1$
$= 1.0$ when $\varepsilon_c/\varepsilon_{cm} \leq 1$

Figure 4 illustrates the modified model with representative experimental data alongside the original Collins model for comparison at ambient temperatures. The analytical curves of the modified Collins model for the stress–strain relationship for GPC

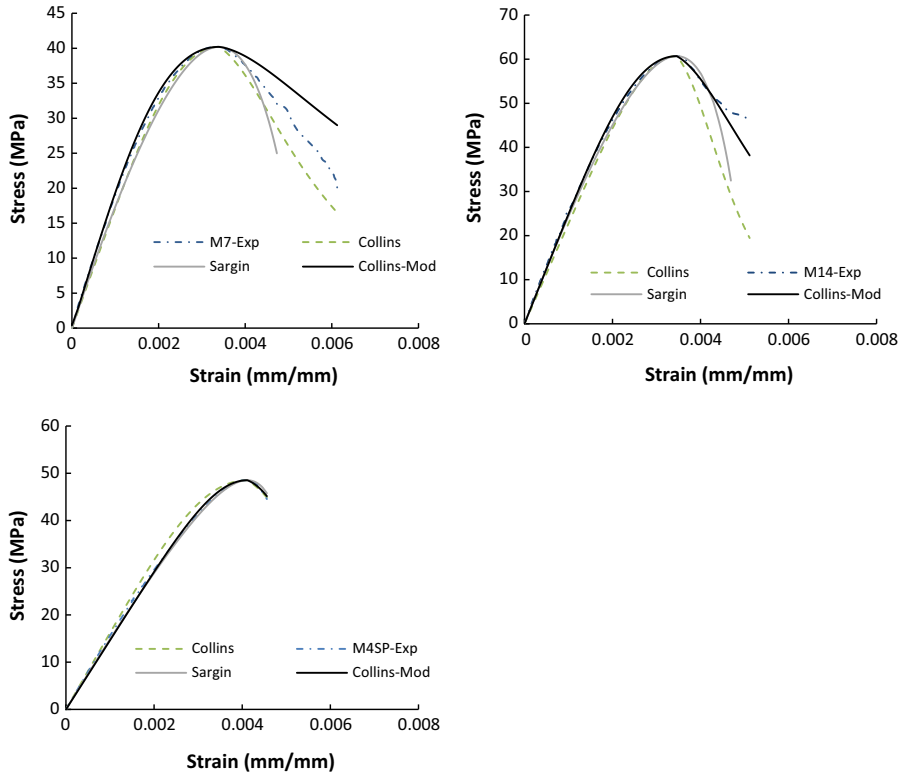

Fig. 4 Comparison of experimental stress strain data (M14, M7 and M4SP) with Collins [37], Sargin [38] and the proposed modified Collins model

concrete improves the behaviour prediction in both pre and post peak stress regions. It may, therefore, be reasonably expected that the modified Collins model is suitable to be used for predicting the stress–strain relationship of GPC concretes.

3.3 Compressive strength at elevated temperatures

Figure 5 shows the evolution of the compressive strength and elastic moduli as a function of the test temperature for all samples. All the samples underwent a decrease in strength between ambient and 200 °C. This initial decline was followed by a moderate to significant gain in strength between 200 and 400 °C. At 800 °C all samples underwent a decrease in strength. Although strength tests were not conducted between 400 and 800 °C, previous research indicates that between these temperatures there is a steady decline in the strength properties of GPC [11, 16, 20, 26]. However, as these tests were not conducted in this temperature range, the presented graph is indicated as a broken line to highlight the uncertainty.

To further investigate the changes in the geopolymer concrete samples with temperature, thermogravimetric analysis (TGA) was undertaken as part of this study. GPC samples containing 413 kg/m^3 of fly ash, 1880 kg/m^3 of aggregates, 56.5 kg/m^3 of 12 M sodium hydroxide solution, 141.3 kg/m^3 of sodium silicate Grade D solution, 14.6 kg/m^3 of free water and 3 kg/m^3 of superplasticizer and viscosity modifier each were used. The preparation and curing conditions for these samples were identical to the ones described earlier. Powdered samples (between 74 and 37 μm) were obtained from these GPC specimens of initial mass ~20 mg and heated to 1050 °C at a heating rate of 10 °C/min for the purpose. It can be seen from Fig. 6 that the GPC sample underwent the most severe loss in mass between 80–200 °C, most likely caused by the escaping water from the system. This observation is corroborated by similar TGA analysis results [11, 12, 15, 18, 28, 39]. This mass loss also coincides with the loss of strength properties in all GPC samples tested here between ambient and 200 °C. It may, therefore, be hypothesized that the loss in strength of GPC samples in this temperature range is due to damage caused by the escaping water. This is also supported by the fact that the mix with the largest water content (M4SP) experienced the greatest strength loss during this exposure range. Moreover, the temperatures are low enough and the exposure time is relatively short, thus limiting the amount of geopolymerization, which may positively impact the strength of GPC concrete.

Between 200 and 400 °C, the increase in the compressive strength of all mixes is attributed mainly to two phenomena: further geopolymerisation and gel stiffening. Between 200 and 300 °C further geopolymerization takes place as ascertained by the differential scanning calorimetry (DSC) results presented by Rahier et al. [39], and the ΔT thermograms of Pan et al. [16]. The exothermic picks noticed by Pan et al. [16] have been proven to be characteristic of geopolymerization [39]. The less pronounced strength gain at temperatures over 300 °C can be attributed to the general stiffening of the geopolymer gel and the removal of moisture from between the gel particles as hypothesized in [16, 40].

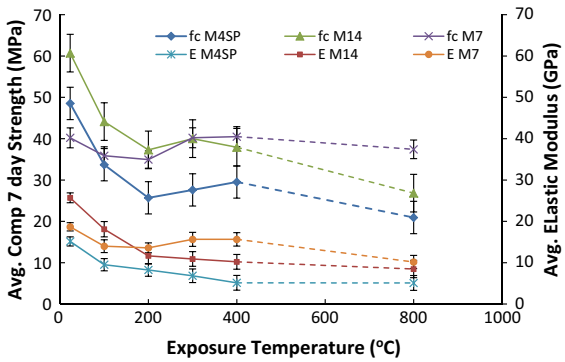

Fig. 5 Evolution of the strength properties as a function of the test temperature. *Dotted lines* are to account for the uncertainty due to lack of data within the range from 400 to 800 °C

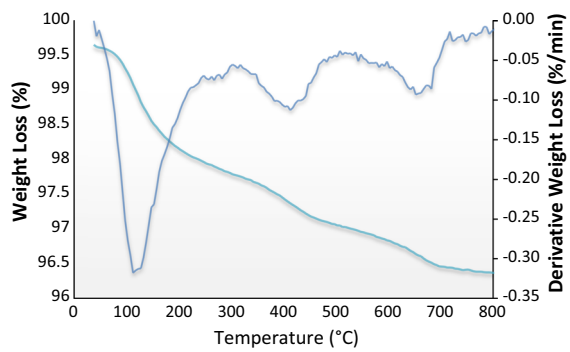

Fig. 6 TGA and DTG curves for GPC concrete

The strength values at 800 °C are rather interesting. For samples M14 and M4SP a sharp decrease in strength is reported (≅45 % of the ambient strength). On the other hand M7 samples experienced a lower loss of strength. This phenomenon may be explained using scanning electron microscopy (SEM). At temperatures of 800 °C and above the un-reacted fly ash particles in the GPC matrix start to diffuse to the boundaries of other particles, which results in their partial fusion [20, 27, 30]. This means that the unused fly ash powder, which is responsible for local weaknesses before exposure, sinters into a stronger solid material within the matrix after exposure. Since M7 has the least amount of alkaline solution it can be hypothesised that, relatively larger amounts of unreacted fly ash is present in these mixes. When exposed to temperature of 800 °C, these particles sinter and form a homogeneous mass, thus resulting in lower loss of strength. This conclusion, however, needs to be further investigated.

3.4 Stress–strain curves at elevated temperatures

Figures 7, 8 and 9 show respectively the stress strain curves for the GPC mixes M7, M14 and M4SP. After the initial strength and stiffness loss up to 200 °C all GPC samples experience a slight gain in strength properties. This may largely be due to geopolymerization of the matrix and to a lesser extent, the expulsion of moisture from the geopolymer gel, as explained in the previous section when discussing the compressive strength. Although desirable, this healing phenomenon makes it impossible at this stage to develop generalized analytical equations for GPC concrete at high temperatures. To develop such a model, the energy of the geopolymerization needs to be quantified at all temperatures. Additionally, the samples tested during this research were virgin samples undergoing their first loading cycles without a sustained pre-loading as would not be the case in a practical structure where sustained stresses are present. By comparison to OPC concrete, for which a sustained stress during heating affects the compressive strength [41], it is hypothesised that a sustained stress during heating would also affect the compressive strength of GPC concrete. To illustrate this point let us hypothesise that a sustained stress of 37 MPa is applied to the M7 sample as shown in Fig. 10. According to the strength envelope obtained without stress during heating, the sample would fail at about

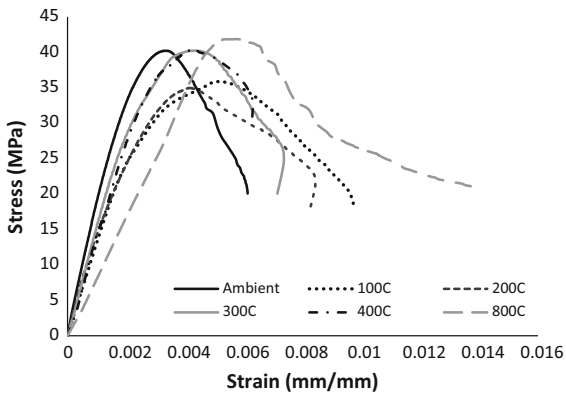

Fig. 7 Stress–strain relationship of M7 samples at high temperatures

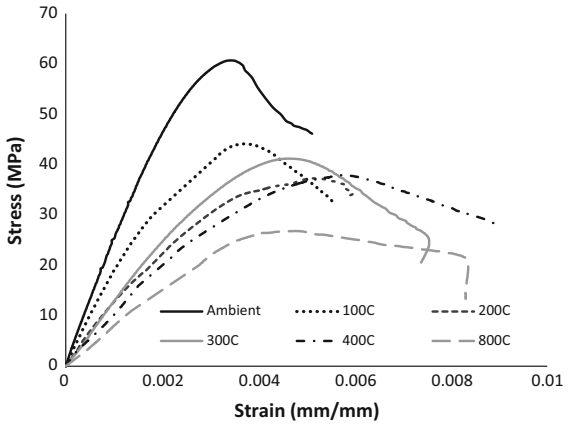

Fig. 8 Stress–strain relationship of M14 samples at high temperatures

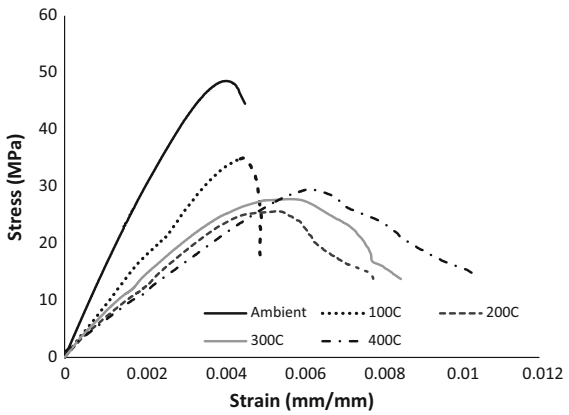

Fig. 9 Stress–strain relationship of M4SP samples at high temperatures

100 °C before 'healing' at around 250 °C. In other words permanent inelastic deformations such as those caused by micro-cracking or crystals sliding (plastic deformations) are recoverable. This, of course, is not physically possible. In the theory of plasticity this is prohibited by the Kuhn–Tucker condition which states that the plastic multiplier must be positive. Similarly in continuum damage mechanics, damage can only increase or remain constant. Otherwise, the second principle of thermodynamics would be violated [42–44]. To develop a generalized analytical model for the stress–strain relationship of GPC concrete at higher temperatures, further testing is required for a variety of pre-load and temperature history.

3.5 Elastic modulus

The evolution of the secant elastic modulus as a function of the exposure temperatures is shown in Fig. 5. The damage to the GPC matrix due to escaping water between test temperatures of 20 and 200 °C, as explained in the earlier section, accounts for the drastic loss of stiffness in this temperature range. For samples M7 and M14 the loss in stiffness is rather slight for temperatures over 200 °C. In fact M7 samples recover almost 10 % of its lost stiffness between 200 and 400 °C. As discussed in the previous section, this minor recovery in the stiffness may be a result of further geopolymerization in the GPC matrix. M7 retains approximately 55 % of its elastic modulus at 800 °C while both M14 and M4SP retained only 35 % of their ambient modulus value. The higher retention of stiffness in M7 samples can be attributed to the recovery of strength properties due to the sintering as explained earlier.

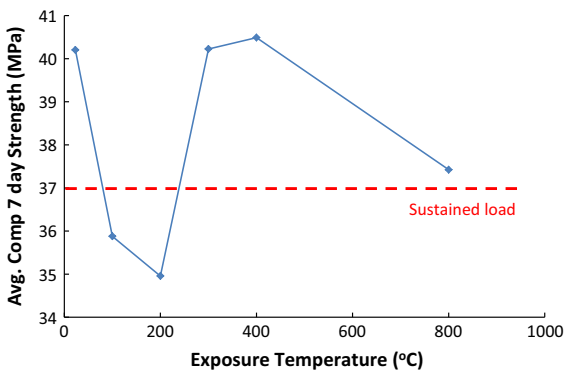

Fig. 10 Illustration of a physically impossible situation

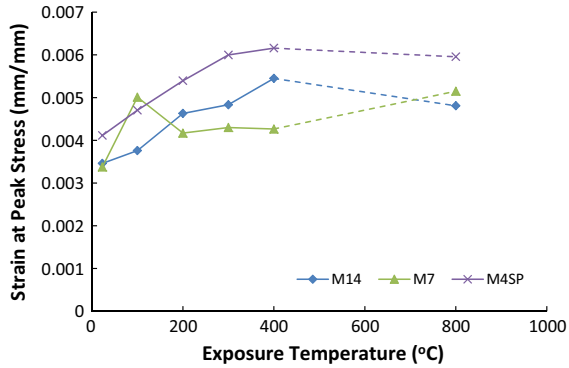

Fig. 11 Variation of the strain at peak stress as a function of the test temperature. *Dotted lines* are to account for the uncertainty due to lack of data within the range from 400 to 800 °C

3.6 Strain at peak stress

The strain at peak stress was also recorded for all the tests. Its variation with the test temperature is shown in Fig. 11. At high temperatures, all the samples displayed a progressively more ductile failure as is evidenced from the relatively large post peak strains developed. Strains at peak stress are in the range of 0.00337 mm/mm (minimum) to 0.006159 mm/mm (maximum). The samples containing Flashag aggregates (M4SP) consistently developed the highest strains at all temperatures. This is most likely due to the fact that Flashag are lightweight aggregates with many voids; hence more compliant.

4 Conclusions

An experimental program to characterise the stress strain behaviour of alkali activated low calcium fly ash concrete at elevated temperatures is discussed. All tested samples underwent a decrease in strength properties between ambient and 200 °C. This strength and stiffness loss may be attributed to the damage caused by the escaping water from the GPC matrix. The escaping water leaves behind numerous voids, thus compromising the structural integrity of the system. TGA of the GPC samples reveals excessive mass loss in this temperature range to support this finding. Between 200 and 400 °C the tested GPC samples, irrespective of the aggregate type used, underwent a slight to significant increase in strength properties, which may be a result of further

geopolymerization. At 800 °C, all samples experienced a loss of strength properties, which may be due to a possible disintegration of the geopolymer gel and/or in the aggregates, as well as to the likelihood of the formation of new phases within the system in the unreacted fly ash or the geopolymer matrix. Progressively ductile failure, demonstrated by relatively large strains at peak stress, was evidenced for all GPC sample as the test temperature was increased. Samples with natural aggregates retained more strength properties as compared to samples with the lightweight Flashag.

It may thus be concluded that established relationships between strength, density and elastic modulus for OPC concrete may not produce realistic results if used for GPC concrete. This discrepancy may lead to erroneous or uneconomical design of structures using GPC concrete. New equations for these quantities are, therefore, proposed for GPC concrete. These have shown good agreement with reported data. Moreover, in the absence of reasonably accurate stress–strain relationship for GPC concrete, engineering and commercial application of such concretes would be very limited. Stress strain models for OPC have been modified to predict the behaviour of GPC concretes. As more data become available, these models can further be improved and form the basis of a generalized analytical model for the stress–strain relationship of GPC. Such a model would be of utmost importance for carrying out numerical analysis of GPC members/structures.

Acknowledgments The authors would like to thank their colleagues at the Department of Civil and Water Engineering, Faculty of Sciences and Engineering, Université Laval, Canada for their support in conducting the Thermogravimetric Analysis testing.

References

1. Davidovits J (1988) Soft mineralogy and geopolymers. In: Proceedings of the geopolymer 88 international conference. France
2. Davidovits J (1989) Geopolymers and geopolymeric materials. J Therm Anal Calorim 35(2):429–441
3. Davidovits J (1991) Geopolymers inorganic polymeric new materials. J Therm Anal 37:1633–1656
4. Lloyd N, Rangan B (2010) Geopolymer concrete with fly ash. In: Second international conference on sustainable construction materials and technologies. Italy
5. Provis J, van Deventer J (2014) Alkali activated materials state-of-the-art report. In: Provis J, van Deventer JSJ (eds) RILEM
6. Fernández-Jiménez A et al (2008) New cementitious materials based on alkali-activated fly ash: performance at high temperatures. J Am Ceram Soc 91(10):3308–3314
7. Bakharev T (2006) Thermal behaviour of geopolymers prepared using class F fly ash and elevated temperature curing. Cem Concr Res 36:1134–1147
8. Rickard W, Temuujin J, van Riessen A (2012) Thermal analysis of geopolymer pastes synthesised from five fly ashes of variable composition. J Non Cryst Solids 358:1830–1839
9. Rickard W, Vickers L, van Riessen A (2013) Performance of fibre reinforced, low density metakaolin geopolymers under simulated fire conditions. Appl Clay Sci 73:71–77
10. Barbosa VF, MacKenzie KJ (2003) Thermal behaviour of inorganic geopolymers and composites derived from sodium polysialate. Mater Res Bull 38(2):319–331
11. Kong D, Sanjayan J (2010) Effect of elevated temperatures on geopolymer paste, mortar and concrete. Cem Concr Res 40:334–339
12. Kong D, Sanjayan J, Sagoe-Crentsil K (2007) Comparative performance of geopolymers made with metakaolin and fly ash after exposure to elevated temperatures. Cem Concr Res 37:1583–1589
13. Guerrieri M, Sanjayan J (2009) Behavior of combined fly ash/slag based geopolymers when exposed to high temperatures. J Fire Mater 34(4):163–175
14. Guerrieri M, Sanjayan J, Collins F (2010) Residual strength properties of sodium silicate alkali activated slag paste exposed to elevated temperatures. Mater Struct 43:765–773
15. Pan Z, Sanjayan J, Rangan B (2009) An investigation of the mechanisms for strength gain or loss of geopolymer mortar after exposure to elevated temperature. J Mater Sci 44(7):1873–1880
16. Pan Z, Sanjayan J (2010) Stress–strain behaviour and abrupt loss of stiffness of geopolymer at elevated temperatures. Cem Concr Compos 32:657–664
17. Shaikh F, Vimonsatit V (2014) Compressive strength of fly-ash-based geopolymer concrete at elevated temperatures. Fire Mater
18. Pan Z, Sanjayan J, Collins F (2014) Effect of transient creep on compressive strength of geopolymer concrete for elevated temperature exposure. Cem Concr Res 56:182–189
19. Rickard WD, Gluth GJ, Pistol K (2016) In-situ thermo-mechanical testing of fly ash geopolymer concretes made with quartz and expanded clay aggregates. Cem Concr Res 80:33–43
20. Junaid MT et al (2014) Aspects of the deformational behaviour of alkali activated fly ash concrete at elevated temperatures. Cem Concr Res 60:24–29
21. Junaid MT, Khennane A, Kayali O (2016) Stress-strain behaviour of alkali activated fly ash concrete at elevated temperatures. In: 2nd international conference on advances in cement and concrete technology in Africa. Tanzania. pp 301–308
22. Junaid MT et al (2015) A mix design procedure for low calcium alkali activated fly ash-based concretes. Constr Build Mater 79:301–310

23. Kayali O (2008) Fly ash lightweight aggregates in high performance concrete. Constr Build Mater 22(12):2393–2399
24. Australian-Standard (1997) AS1012.17-1997: determination of static chord modulus of elasticity and poissons ratio of concrete specimens. In: Methods of testing concrete
25. Australian-Standard (1999) AS 1010.9-1999: Determination of the compressive strength of concrete specimens. In: Methods of testing concrete
26. Junaid MT, Khennane A, Kayali O (2014) Investigation into the effect of the duration of exposure on the behavior of geopolymer concrete at elevated temperatures. In: MATEC web of conferences. p 11
27. Junaid MT, Khennane A, Kayali O (2014) Performance of fly ash based geopolymer concrete made using non-pelletized fly ash aggregates after exposure to high temperatures. Mater Struct
28. Kong D, Sanjayan J (2008) Damage behavior of geopolymer composites exposed to elevated temperatures. Cement Concr Compos 30:986–991
29. Duxson P, Lukey G, van Deventer JS (2006) Thermal evolution of metakaolin geopolymers: part 1—physical evolution. J Non Cryst Solids 352:5541–5555
30. Škvára F, Jílek T, Kopecký L (2005) Geopolymer materials based on fly ash. Ceram Int 49(3):195–204
31. RILEM (1997) Test methods for mechanical properties of concrete at high temperatures. Recommendations part 6: thermal strains. In: TC 129-MHT. 1997. pp 17–21
32. Diaz-Loya EI, Allouche E, Vaidya S (2011) Mechanical properties of fly-ash-based geopolymer concrete. ACI Mater J 108(3):300–306
33. Yifei C (2015) Bond behaviour between reinforcing steel bars and fly-ash based geopolymer concrete. School of Engineering and Information Technology, University of New South Wales, Canberra
34. Ponce V, Perez F. *VLab: online regression*, S.D.S. Univeristy, Editor
35. Anderberg Y, Thelandersson S (1976) Stress and deformation charactersistics of concrete, 2 experimental investigations and materail behaviour model. Bulletin 54, 1976. University of Lund, Sweden
36. Tomaszewicz A (1984) *Betongens Arbeidsdiagram*, Trondheim, Editor, SINTEF Report No 65A84065
37. Collins MP, Mitchell D, MacGregor JG (1993) Structural design considerations for high-strength concrete. Concr Int 15(5):27–34
38. Sarjin M (1971) Stress-strain relationships for concrete and the analysis of structural concrete sections. In: Solid mechanics division. Universtity of Waterloo, Canada
39. Rahier H, van Mele B, Wastiels J (1996) Low-temperature synthesized aluminosilicate glasses. Part II rheological transformations during low-temperature cure and high-temperature properties of a model compound. J Mater Sci 31(1):80–85
40. Cheng F-P, Kodur V, Wang T-C (2004) Stress-strain curves for high strength concrete at elevated temperatures. J Mater Civ Eng 16(1):84–90
41. Khennane A, Baker G (1993) Uniaxial model for concrete under variable temperature and stress. J Eng Mech 119(8):1507–1525
42. Khennane A, Baker G (1992) Plasticity models for the behaviour of concrete at elevated temperatures. Part 1: failure criterion. Comput Methods Appl Mech Eng 10(2):207–223
43. Khennane A, Baker G (1992) Plasticity models for the behaviour of concrete at elevated temperatures. Part 2: implementation and simulation tests. Comput Methods Appl Mech Eng 100(2):225–248
44. Khennane A, Baker G (1992) Thermo-plasticity model for concrete under varying temperature and biaxial stress. R Soc A